ÉCOLE POLYTECHNIQUE
FÉDÉRALE DE LAUSANNE

MATHICSE
Mathematics Institute of Computational Science and Engineering
School of Basic Sciences - Section of Mathematics

MATHICSE Technical Report
Nr. 7.2012
February 2012

Connecting ventricular assist devices to the aorta : a numerical model

Jean Bonnemain, Simone Deparis and Alfio Quarteroni

http://mathicse.epfl.ch

Phone: +41 21 69 37648

Address:
EPFL - SB - MATHICSE (Bâtiment MA)
Station 8 - CH-1015 - Lausanne - Switzerland

Fax: +41 21 69 32545

Connecting Ventricular Assist Devices to the Aorta: a Numerical Model

J. Bonnemain, S. Deparis, A. Quarteroni

Abstract Mechanical circulatory support, in particular ventricular assist devices (VAD), has been recently proposed as an alternative to transplantation in the treatment of terminal heart failure in the context of the lack of donors and raising number of patients on the waiting list. Although these systems have proved their efficiency through a rigorous patient selection, the complication rate remains high and experience shows that many of them are related to haemodynamic modifications due to VAD implantation. Furthermore, VAD themselves have been widely studied, while the flow near the anastomosis VAD-aorta is still not well-known, although many complications arise at this site. We present here the mathematical settings and some preliminary results of a numerical model of the anastomosis between the outflow cannula of left ventricular assist devices (LVAD) and the aorta.

Jean Bonnemain
CMCS - MATHICSE - EPFL, Lausanne, Switzerland e-mail: jean.bonnemain@epfl.ch
Cardiovascular Surgery Department, CHUV, Lausanne, Switzerland

Simone Deparis
CMCS - MATHICSE - EPFL, Lausanne, Switzerland e-mail: simone.deparis@epfl.ch

Alfio Quarteroni
CMCS - MATHICSE - EPFL, Lausanne, Switzerland e-mail: alfio.quarteroni@epfl.ch
MOX, Politecnico di Milano, Milano, Italy

1 Introduction - The Clinical Problem

Heart failure is a clinical syndrome that expresses the inability of the heart to provide enough blood to the organs in order to satisfy their metabolic needs. In other terms, the pump is failing. The causes of heart failure are numerous (coronary artery disease and myocardial infarction, valvular disease, cardiomyopathy, myocarditis, to mention a few) as well as their symptoms (e.g. dyspnea, fatigue, peripheral edema) [8].

Within the population studied by the European Society of Cardiology (>900 million people in 51 countries), heart failure prevalence is around 2-3% and affects at least 15 millions patients [4]. In the USA, 2.5% of the adult population (5.7 million people) suffer from heart failure and 670'000 new cases occur each year. Furthermore, prevalence is higher in the elderly - 6-10% of people older than 65 years. Among the deaths reported in 2004, 292'000 were caused directly or indirectly by heart failure. The estimated overall cost of heart failure in the USA in 2009 was 37.2 billion dollars [10].

The first line of the treatment of heart failure includes lifestyle modifications, like sodium and fluid restriction, smoking cessation or weight loss. These are necessary but usually not sufficient. The second line of treatment is the use of drugs, like angiotensin-converting enzyme (ACE) inhibitors, angiotensin-receptor blockers, diuretics and β-blockers. Finally, invasive treatment includes cardiac resynchronisation therapy, that consists in the implantation of a pacemaker (biventricular pacing, with or without implantable cardioverter defibrillator) and transplantation [14]. However, heart donors are scarce (2210 transplantations in 2007 in the USA) and, in June 2008, 2607 patients were still on the waiting list [10]. An alternative approach has been recently suggested in order to compensate the lack of donors and to provide a treatment for terminal heart failure: the *mechanical circulatory support*.

Various types of mechanical circulatory support exist with different clinical indications, but their goal is always the same: assist (or replace) the pump function of the heart. They are classified as follows:

- Intra-Aortic Balloon Pump (IABP)
- Extracorporeal Membrane Oxygenation (ECMO)
- Ventricular Assist Devices (VAD)
- Total Artificial Heart (TAH)

IABP and ECMO are short-term assist devices (hours to days) while VAD and TAH have an intermediate or long-term use (days to years). Depending on the indications, they can be considered as:

- *Bridge to transplantation*, for patients on waiting list;
- *Bridge to recovery*, as temporary circulatory support;
- *Bridge to decision*, gives time to the clinician to find the best therapeutic option;
- *Bridge to eligibility*, for patients initially ineligible for transplantation who become eligible after VAD implantation, due to the normalization of several clinical parameters;

- *Destination therapy*, for patients who are ineligible for transplantation [20].

In this paper, we will focus on Ventricular Assist Devices (VAD) (see Fig. 1). They can assist right, left or both sides of the heart, according to the underlying pathology. Furthermore, they can deliver pulsatile or non-pulsatile flows, and they can be paracorporeal, partially or totally implantable. It is important to notice that newer, smaller, continuous flow pumps (e.g. see Fig 2) showed better results, as reduction of complications, durability and mortality [21].

Fig. 1: The VAD HeartMate II. Reprinted with the permission of Thoratec Corporation.

All these systems have proved their efficiency through a rigorous patient selection. However, the complication rate remains high, e.g. [7], in particular they may take the following form:

- Bleeding (30%);
- Thromboembolism (3-35%);
- Infections (18-59%);
- Right ventricular failure (20-30%);
- Primary device failure (6% at 6 months to 64% at 2 years).

VAD as a *destination therapy* showed clinical benefits [20], however there is still room for better outcomes and for a reduction of the costs, which, for the time being, remain high [1].

As mentioned before, complications remain a major issue. Many of them are related to haemodynamic modifications due to the VAD implantation. In fact, abnormalities in flow and shear patterns can lead to platelet activation and to the for-

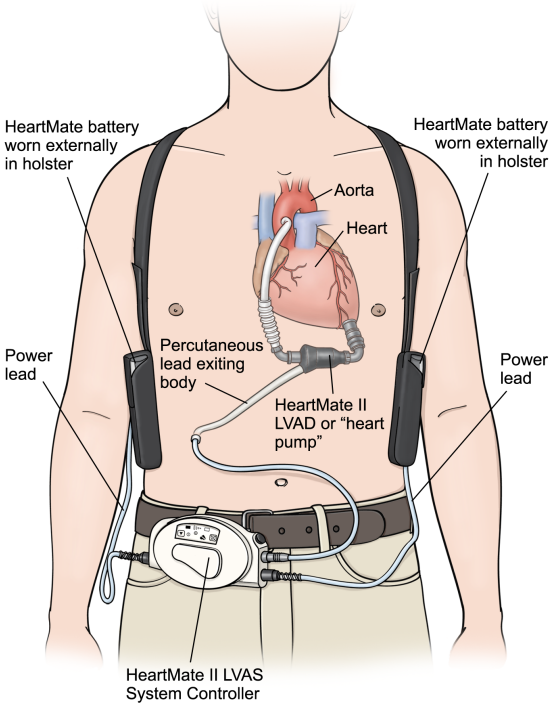

Fig. 2: Left Ventricle Assist Device, Reprinted with the permission of Thoratec Corporation. The inflow cannula is inserted in the apex of the deficient ventricle and the outflow cannula is anastomosed to the ascending aorta. Blood flow exits the ventricle through the inflow cannula, is actively pumped by the pumping chamber and goes through the outflow cannula to the aorta. A percutaneous drive line carries the electrical cable to the battery packs and electronic controls.

mation of clots. In particular, regions of turbulent flow, recirculation and stagnation have a high thrombogenicity. Finally, subsequent shear stress distribution on the arterial wall can have short term negative effects (e.g. thrombus formation) and in the long-term has an impact on arterial remodeling and atherosclerosis [13]. While VAD themselves have been widely studied, e.g. [23] and [15], the flow near the anastomosis VAD-aorta is still not well-known, although many complications arise at this site.

2 Methods and Results

The main motivation of this work is to describe a mathematical model that allows a better understanding of the flow behavior occuring in the anastomotic region between the VAD and the aorta. When creating a numerical model, especially with patient-specific data, the procedure comprises three stages:

- *pre-processing* (before the numerical simulation)
  - data acquisition (DICOM images),
  - geometry construction,
  - mesh generation;
- *processing* (numerical simulation itself)
  - set-up of mathematical equations for blood motion,
  - set-up of numerical algorithms,
  - parallel execution;
- *post-processing* (after the numerical simulation)
  - analysis of results
  - model validation.

A short description follows.

2.1 Pre-processing

For patients under ventricular assistance, the most frequent image acquisition method is *CT-scan* (computed tomography), because it is fast and vessels can be seen using intravenous contrast. CT-scan uses X-rays that provide a set of bidimensional images (slices) of a given region of the body (e.g. thorax, see Fig 3).

Unfortunately, the presence of the device, due to its metallic components, induces a lot of noise and artifacts on images (See Fig. 4). Consequently the geometry of the region of interest (outflow cannula of the LVAD, aorta and its branches) cannot be reconstructed directly on the native image (this would indeed produce an aberrant geometry). Therefore the images need to be cleaned by filters of various kind.

Treatment of images is performed by reducing the level window (i.e. focusing only on a defined grey range) and enhancing the contrast of the greyscale image using contrast-limited adaptive histogram equalization. In particular this filter allows to enhance the differences between the vessel with contrast (the region of interest) and the surrounding tissues (to be neglected in the segmentation). Then a gradient anisotropic diffusion filter is applied to reduce the noise, resulting in a smoothed image. Fig. 5 shows these different filters.

Having convenient images for segmentation, the geometry of the region of interest can be reconstructed. The gradient of the previously treated images is then

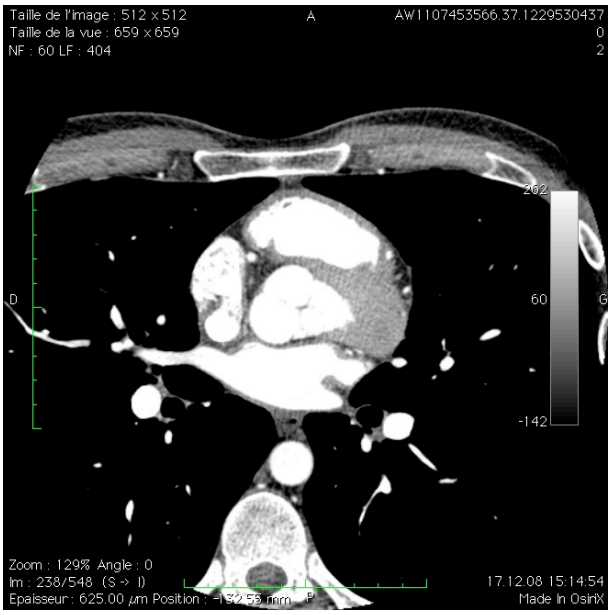

Fig. 3: Example of a CT-scan image at the level of the aortic valve.

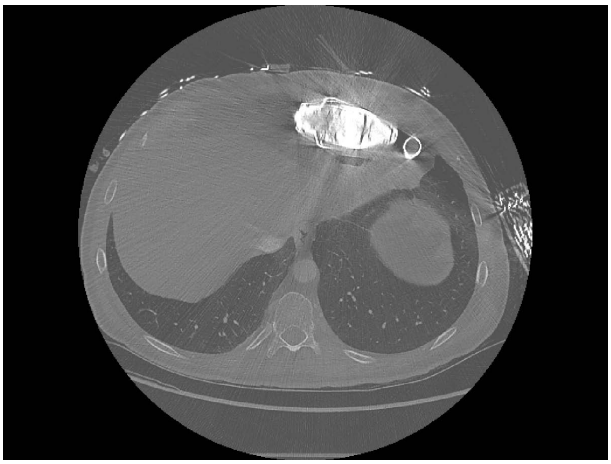

Fig. 4: CT-scan slice of a patient with a continuous flow LVAD at the level of the LVAD itself. On the top of the image, the VAD itself and the inflow cannula that connects the left ventricle to the LVAD. Note the noise and artifacts induced by the presence of the device.

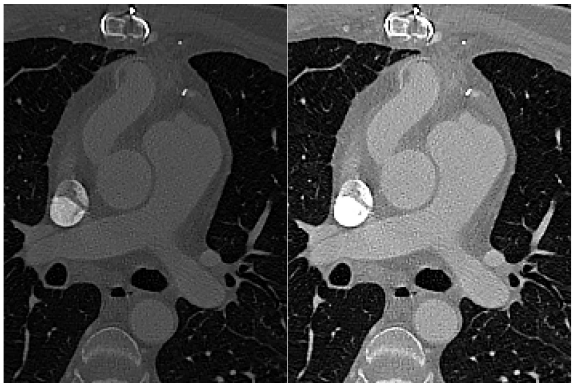

(a) Native image (b) Reduced level window

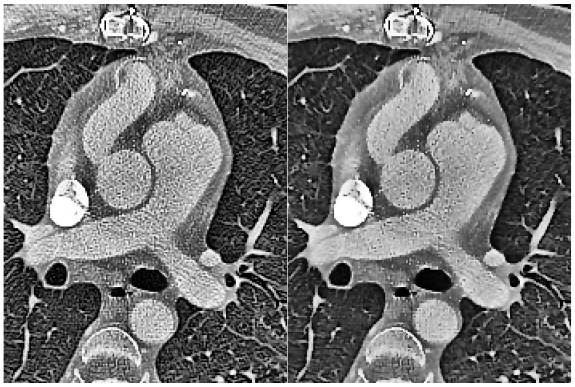

(c) Enhanced image (d) Denoised image

Fig. 5: Effects of the different filters applied to the DICOM images, seen at the level of the anastomosis between the outflow cannula of the LVAD and the aorta.

calculated and the watershed segmentation algorithm [22] is applied to the result. To improve the obtained segmentation, mathematical morphology filters are then performed and the final surface is extracted. All these steps are performed using the InsightToolKit library[1]. These methods allow to reconstruct only the geometry of the fluid, i.e., the volume inside the artery corresponding to the blood (the lumen). The arterial wall itself is usually not seen on DICOM images like CT-scan or MRI, consequently its geometry cannot be directly reconstructed. Since we want to perform numerical simulations that takes into account arterial wall deformation (i.e. the so-called Fluid-Structure Interaction, FSI), we have to artificially reconstruct the arterial wall, assuming that arterial wall thickness is proportional to the local vessel radius [9].

[1] www.itk.org

Finally we used the library vmtk[2] to create meshes for the fluid (blood) and structure (arterial wall, outflow cannula) and to a-priori identify the boundary layers.

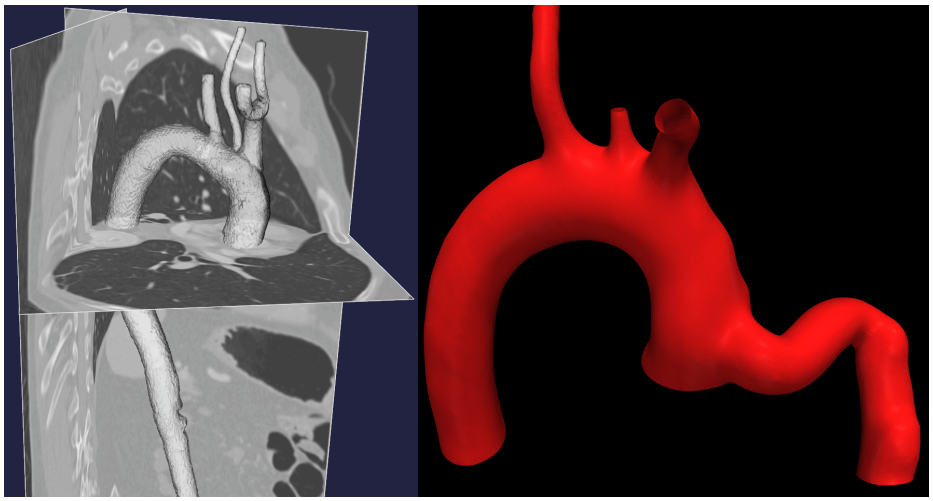

(a) Geometry of an healthy aorta obtained from a CT-scan exam.

(b) Geometry of the fluid domain (the lumen).

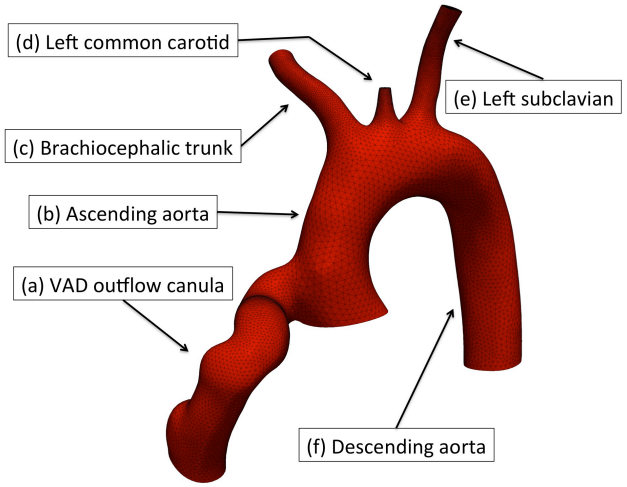

(c) Grid of the fluid domain.

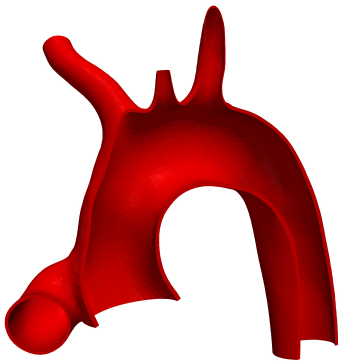

(d) Grid of the arterial wall.

Fig. 6: Geometry and computational grids.

[2] www.vmtk.org

2.2 Processing

We aim at modeling the flow in the whole computational domain in Fig. 6 (comprising (a) cannula, (b) ascending aorta, (c) brachiocephalic trunk, (d) left common carotid, (e) left subclavian, (f) descending aorta) by a fluid-structure coupled problem. More precisely, the blood flow in the lumen is described by the Navier-Stokes equations for a Newtonian fluid in the Arbitrary Lagrangian Eulerian (ALE) frame of reference [16], while the arterial wall is modeled by a 3D elastodynamic equation. The same model is adapted for the artifical cannula (which is made of woven polyester), the only difference in our model being represented by a larger Youg modulus, corresponding to a higher stiffness.

Let Ω_f and Ω_s be the reference domain for the fluid and the structure, respectively, and $\Gamma_{FSI} = \partial\Omega_f \cap \partial\Omega_s$ the fluid-structure interface. In the case at hand, $\Omega_f(t)$ is in fact the lumen of the whole domain in Fig. 6 (comprising the cannula, the aorta and its branches) whereas $\Omega_s(t)$ indicates the arterial and cannula walls. At every time $t > 0$, the current configuration of the fluid domain, $\Omega_f(t)$, is given by the ALE map

$$\begin{aligned} \mathscr{A}_t : \Omega_f &\to \Omega_f(t) \\ \mathbf{x} &\to \mathscr{A}_t(\mathbf{x}) = \mathbf{x} + \mathbf{d}_f(x), \end{aligned}$$

where $\mathbf{d}_f$ is the displacement of the fluid domain, therefore $\Omega_f(t) = \mathscr{A}_t(\Omega_f, t)$. Practically $\mathbf{d}_f = Ext(\mathbf{d}_s|_{\Gamma_{FSI}})$, where $\mathbf{d}_s$ is the solid displacement and the extension $Ext(\cdot)$ is an harmonic lifting (or extension) operator from Γ_{FSI} to Ω_f (see [6]).

The Navier-Stokes equations are coupled with a linear elastic model describing the structure's behavior [6]. The partial differential equations modeling the fluid and the structure are:

$$\begin{cases} \rho_f \partial_t \mathbf{u} + \rho_f(\mathbf{u} - \mathbf{w}) \cdot \nabla \mathbf{u} - \nabla \cdot \sigma_f = 0 & \text{in } \Omega_f(t), \\ \nabla \cdot \mathbf{u} = 0 & \text{in } \Omega_f(t), \end{cases}$$

$$\rho_s \partial_{tt} \mathbf{d}_s - \nabla \cdot \Pi = 0 \quad \text{in } \Omega_s,$$

and the coupling at the fluid-structure interface is expressed by the continuity of the velocity, the equilibrium of the stresses, and the geometric adherence:

$$\begin{cases} \mathbf{u} = \partial_t \mathbf{d}_s & \text{on } \Gamma_{FSI}(t), \\ \Pi \mathbf{n}_s = -J_f \sigma_f(\mathbf{F}_f)^{-T} \mathbf{n}_f & \text{on } \Gamma_{FSI}, \\ \mathbf{d}_f = Ext(\mathbf{d}_s|_{\Gamma_{FSI}}), \quad \mathbf{w} = \partial_t \mathbf{d}_f & \text{in } \Omega_f, \end{cases}$$

Here: $\mathbf{u} = \mathbf{u}(\mathbf{x}, t)$ is the fluid velocity, $p = p(\mathbf{x}, t)$ the pressure, $\mathbf{w} = \mathbf{w}(\mathbf{x}, t) = \partial_t \mathbf{d}_f$ the domain velocity; ∂_t the partial derivative with respect to the time; ρ_f and ρ_s the fluid and solid densities; $\sigma_f = \sigma_f(\mathbf{u}, p) = -p\mathbf{I} + \mu\varepsilon(\mathbf{u})$ the fluid Cauchy stress tensor, μ the fluid dynamic viscosity, $\varepsilon(\mathbf{u}) = (\nabla\mathbf{u} + \nabla\mathbf{u}^T)/2$ the strain rate tensor, and $\Pi = \Pi(\mathbf{d_s})$ the first Piola-Kirchhoff stress tensor of the structure. Moreover $\mathbf{F}_f = \nabla\mathscr{A}_t$ is the fluid domain gradient of deformation, $J_f = \det \mathbf{F}_f$ the jacobian, $\mathbf{n}_f$ and $\mathbf{n}_s$ the

outward unit normals to the fluid and solid domains. Additional condititions on the external boundary are necessary to close the equations.

Regarding the numerical approximation, we use here a geometry-convective explicit (GCE) time discretization of the 3-D FSI problem [3]. It means that both the convective field and the fluid computational domain are extrapolated from the previous time step. The other terms are treated with a first order backward Euler scheme. These equations are discretized in space by a $\mathbb{P}_1$-$\mathbb{P}_1$ Finite Element method stabilized by interior penalty. This implies that the Navier-Stokes equations are reduced to a linear problem at each time step. The equations for the structure are also linear, requiring no special treatment. Due to the explicit treatment of the geometry, the discrete coupled problem is linear. It can therefore be solved by a GMRES method preconditioned by overlapping algebraic Schwarz preconditioners based on an inexact block factorization of the system (see [3]).

The software used is based on LifeV (www.lifev.org), a parallel finite element (FE) library providing implementations of state-of-the-art mathematical and numerical methods. It has been used already in medical and industrial marks to simulate fluid structure interaction and mass transport processes [3]. The kind of simulations we are interested in are very heavy in term of computational costs, therefore supercomputers like the Blue Gene/P (IBM) or Cray XT or XE series are necessary [2].

2.3 Post-processing

Post-processing of the data is also an important issue since the solutions given by the simulations are heavy in terms of data size. Therefore critical parameters have to be carefully identified in order to provide a relevant and meaningful analysis of the results both from the mathematical and clinical points of view. Their description with respect to the model that is applied is made in chapter 3. We used ParaView [3] to perform the post-processing of the data. It allows to analyze results both in a qualitative (e.g. flow pattern at a given location) and quantitative manner (flowrate at a given vessel).

Finally the model has to be validated. We are currently performing *in vitro* validation. It is conducted by comparing values obtained with the *in vitro* model with the *in silico* one, based on the same geometries and input parameters, using the PIV (Particle Image Velocimetry) method.

[3] www.paraview.org

3 Results

We present here preliminary results of our numerical simulations. On a background of a network made of the coupling of 1D models for the systemic vasculature [5], [11], and [19], we overlay a 1D model for the cannula on the ascending aorta. This model has the advantage to have a low computational cost; simulating 6 heartbeats takes typically 8 hours using 8 processors (64 CPU hours). It also allows to evaluate the systemic effects of the LVAD. As a drawback it cannot evaluate local tridimensional features, e.g., the zones of flow recirculation or stagnation at the anastomosis site, nor the charge loss due to the anastomosis. Fig. 7 shows the flowrate and pressure at several critical arteries. Note that it is possible to evaluate pressure and flowrate at the main arteries.

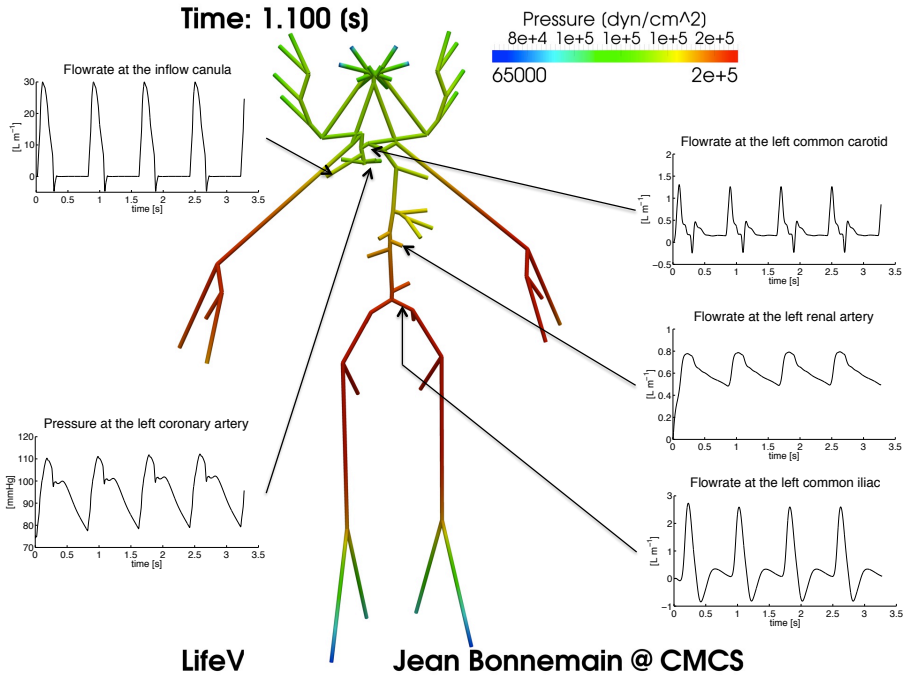

Fig. 7: Arterial tree model composed by 1D elements.

We then enrich our model by using a 3D model of the region depicted in Fig. 6 comprising the connection of the outflow cannula, the aorta and its branches. Its coupling with a 1D model of the entire cardiovascular system (see Fig.8) yields a geometric multiscale model [11], [12], [18], and [17]. The advantages of using such

a multiscale model are numerous. In particular it is possible to evaluate the local effects of the insertion of the LVAD (with the 3D model) and evaluate its interaction with the cardiovascular system (with the coupling with the 1D model). The drawback is its elevated computational cost. E.g., using 64 cores on an IBM Intel Nehalem cluster composed by blades containing two quad-core 2.66 GHz nodes each, takes 72 hours to simulate 3 heartbeats (corresponding to as many as 4608 CPU hours). In particular, Fig. 10 shows secondary flows and stagnation zones in the region of anastomosis. In this case the aortic valve is closed and all the inflow comes from the cannula of the LVAD.

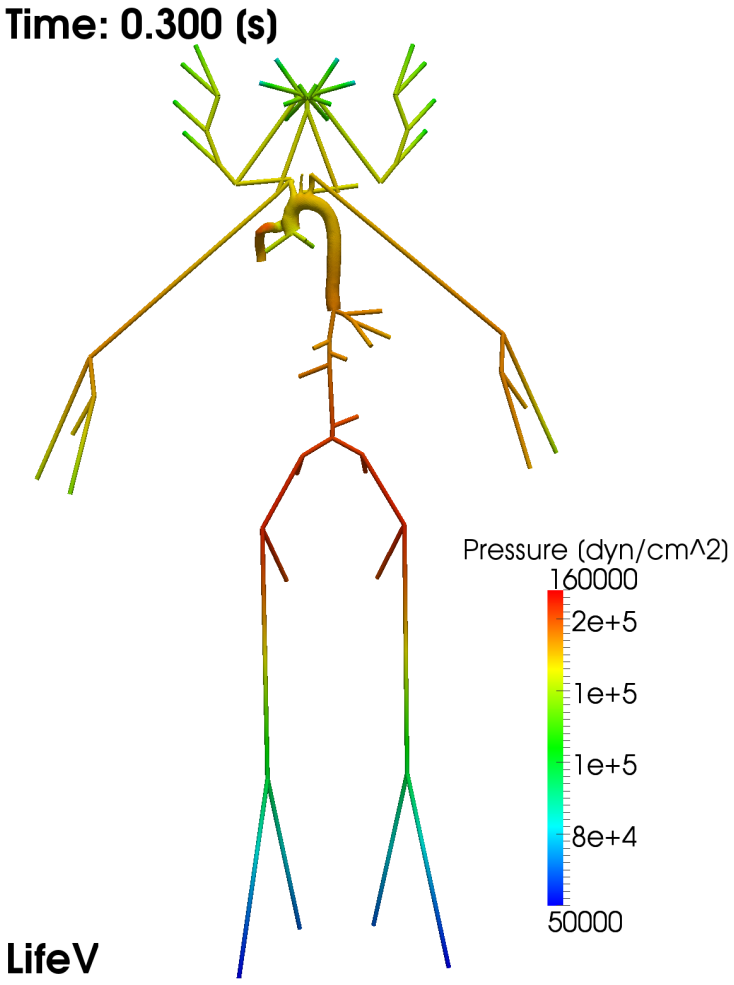

Fig. 8: Multiscale model. Arterial tree composed by a 3D FSI model for the domain of Fig. 6 and by 1D elements for the remaining circulation.

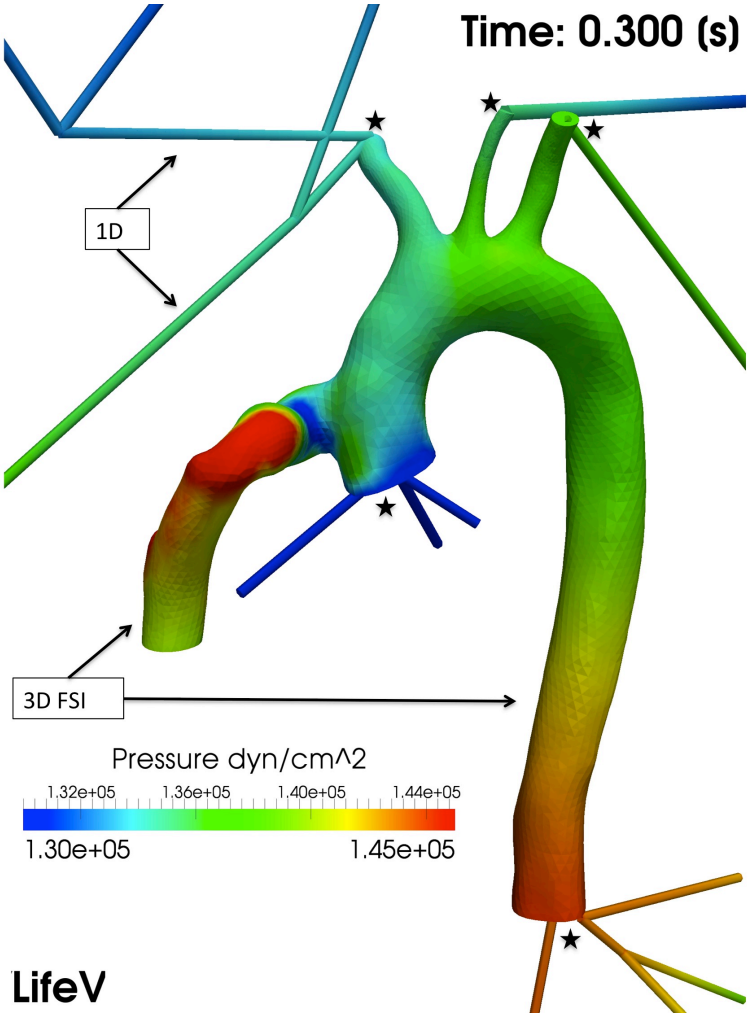

Fig. 9: Multiscale model. Focus on the 3D FSI model and its coupling with 1D elements. The stars denote the coupling interfaces.

4 Conclusion

This work represents the first step towards a clinical tool for patient-specific optimized VAD implantation. In that sense, we join the idea of the well-known expression: *from bench to bedside*.

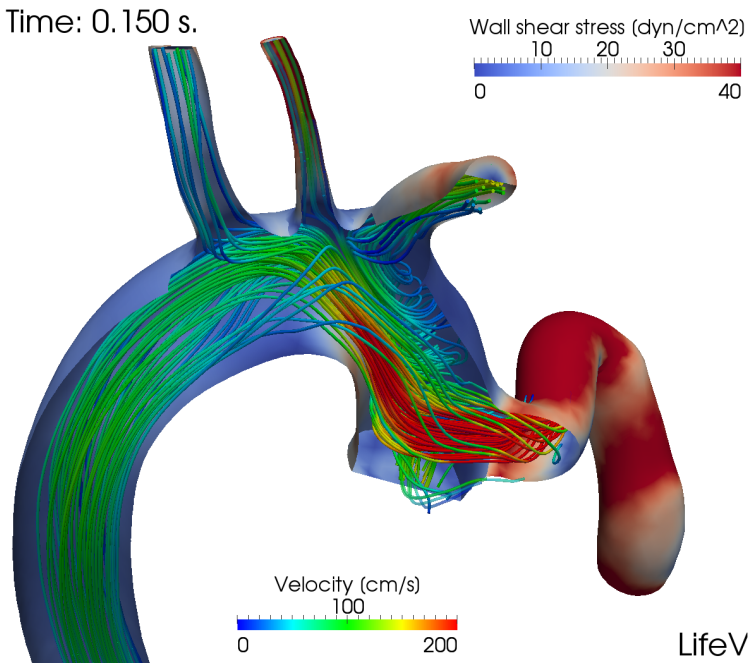

Fig. 10: Multiscale model. Focus on the 3D model showing the streamlines and the wall shear stress distribution (WSS), posterior view.

More specifically in this study we have focused on the anastomosis of LVAD to the aorta. The techniques we developed allow us to run patient-specific simulations giving the opportunity to understand the behavior of the blood flow near the anastomosis and the interaction between LVAD and the cardiovascular system in a complete non-invasive way. In the long run, hopefully this will open the way to predictive surgery.

Acknowledgements

We acknowledge Cristiano Malossi for having provided the multiscale framework and for his valuable help to set up the numerical simulations. We also thank Prof. Ludwig Karl von Segesser for his advice, especially in the clinical field. Finally we are grateful to Elena Faggiano and Paolo Crosetto for the help they provided, the Swiss National Fund grant 323630-133898, the European Research Council Advanced Grant, Mathcard, Mathematical Modelling and Simulation of the Cardiovascular System, Project ERC-2008-AdG 227058, and the entire LifeV community.

References

1. Clegg, A., Scott, D., Loveman, E., Colquitt, J., Royle, P., Bryant, J.: Clinical and cost-effectiveness of left ventricular assist devices as destination therapy for people with end-stage heart failure: a systematic review and economic evaluation. International journal of technology assessment in health care **23**(2), 261–8 (2007)
2. Crosetto, P., Deparis, S., Fourestey, G., Quarteroni, A.: Parallel algorithms for fluid-structure interaction problems in haemodynamics **33**(4), 1598–1622 (2011)
3. Crosetto, P., Reymond, P., Deparis, S., Kontaxakis, D., Stergiopulos, N., Quarteroni, A.: Fluid-structure interaction simulation of aortic blood flow. Computers and Fluids **43**(1), 46–57 (2011)
4. Dickstein, K., Cohen-Solal, A., Filippatos, G., McMurray, J.J.V., Ponikowski, P., Poole-Wilson, P.A., Strömberg, A., van Veldhuisen, D.J., Atar, D., Hoes, A.W., Keren, A., Mebazaa, A., Nieminen, M., Priori, S.G., Swedberg, K., for Practice Guidelines, E.C., Vahanian, A., Camm, J., Caterina, R.D., Dean, V., Dickstein, K., Filippatos, G., Funck-Brentano, C., Hellemans, I., Kristensen, S.D., McGregor, K., Sechtem, U., Silber, S., Tendera, M., Widimsky, P., Zamorano, J.L., Reviewers, D., Tendera, M., Auricchio, A., Bax, J., Böhm, M., Corrà, U., Bella, P.D., Elliott, P.M., Follath, F., Gheorghiade, M., Hasin, Y., Hernborg, A., Jaarsma, T., Komajda, M., Kornowski, R., Piepoli, M., Prendergast, B., Tavazzi, L., Vachiery, J.L., Verheugt, F.W.A., Zamorano, J.L., Zannad, F.: Esc guidelines for the diagnosis and treatment of acute and chronic heart failure 2008. Eur Heart J **29**(19), 2388–442 (2008)
5. Formaggia, L., Lamponi, D., Quarteroni, A.: One-dimensional models for blood flow in arteries. Journal of Engineering Mathematics **47**, 251–276 (2003)
6. Formaggia, L., Quarteroni, A., Veneziani, A. (eds.): Cardiovascular Mathematics: Modeling and Simulation of the Circulatory System, *Modeling, Simulation and Applications*, vol. 1. Springer, Milan (2009)
7. Gordon, R., Quagliarello, B., Lowy, F.: Ventricular assist device-related infections. The Lancet Infectious Diseases **6**(7), 426–437 (2006)
8. Jessup, M., Brozena, S.: Heart failure. N Engl J Med **348**(20), 2007–18 (2003)
9. Langewouters, G.J.: Visco-elasticity of the human aorta in vitro in relation to pressure and age. Ph.D. thesis, Free University, Amsterdam (1982)
10. Lloyd-Jones, D., Adams, R., Carnethon, M., Simone, G.D., Ferguson, T.B., Flegal, K., Ford, E., Furie, K., Go, A., Greenlund, K., Haase, N., Hailpern, S., Ho, M., Howard, V., Kissela, B., Kittner, S., Lackland, D., Lisabeth, L., Marelli, A., Mcdermott, M., Meigs, J., Mozaffarian, D., Nichol, G., O'donnell, C., Roger, V., Rosamond, W., Sacco, R., Sorlie, P., Stafford, R., Steinberger, J., Thom, T., Wasserthiel-Smoller, S., Wong, N., Wylie-Rosett, J., Hong, Y.: Heart disease and stroke statistics–2009 update: A report from the american heart association statistics committee and stroke statistics subcommittee. Circulation **119**(3), e21–e181 (2009)
11. Malossi, A.C.I., Blanco, P.J., Deparis, S.: A two-level time step technique for the partitioned solution of one-dimensional arterial networks (2011). Submitted
12. Malossi, A.C.I., Blanco, P.J., Deparis, S., Quarteroni, A.: Algorithms for the partitioned solution of weakly coupled fluid models for cardiovascular flows. International Journal for Numerical Methods in Biomedical Engineering (2011)
13. May-Newman, K., Hillen, B., Sironda, C., Dembitsky, W.: Effect of lvad outflow conduit insertion angle on flow through the native aorta. Journal of Medical Engineering & Technology **28**(3), 105–9 (2004)
14. Mcmurray, J., Pfeffer, M.: Heart failure. The Lancet **365**(9474), 1877–1889 (2005)
15. Medvitz, R., Kreider, J., Manning, K., Fontaine, A., Deutsch, S., Paterson, E.: Development and validation of a computational fluid dynamics methodology for simulation of pulsatile left ventricular assist devices. ASAIO Journal **53**(2), 122–131 (2007)
16. Nobile, F.: Numerical approximation of fluid-structure interaction problems with application to haemodynamics. Ph.D. thesis, École Polytechnique Fédérale de Lausanne (2001)
17. Passerini, T., de Luca, M., Formaggia, L., Quarteroni, A., Veneziani, A.: A 3D/1D geometrical multiscale model of cerebral vasculature. Journal of Engineering Mathematics **64**(4), 319–330 (2009)

18. Quarteroni, A., Veneziani, A.: Analysis of a geometrical multiscale model based on the coupling of PDE's and ODE's for blood flow simulations. Multiscale Modeling & Simulation **1**(2), 173–195 (2003)
19. Reymond, P., Merenda, F., Perren, F., Rufenacht, D., Stergiopulos, N.: Validation of a one-dimensional model of the systemic arterial tree. Am J Physiol Heart Circ Physiol **297**(1), H208–222 (2009)
20. Rose, E.A., Gelijns, A.C., Moskowitz, A.J., Heitjan, D.F., Stevenson, L.W., Dembitsky, W., Long, J.W., Ascheim, D.D., Tierney, A.R., Levitan, R.G., Watson, J.T., Meier, P., Ronan, N.S., Shapiro, P.A., Lazar, R.M., Miller, L.W., Gupta, L., Frazier, O.H., Desvigne-Nickens, P., Oz, M.C., Poirier, V.L., of Mechanical Assistance for the Treatment of Congestive Heart Failure (REMATCH) Study Group, R.E.: Long-term mechanical left ventricular assistance for end-stage heart failure. N Engl J Med **345**(20), 1435–43 (2001)
21. Slaughter, M., Rogers, J., Milano, C., Russell, S., Conte, J., Feldman, D., Sun, B., Tatooles, A., Delgado III, R., Long, J., Wozniak, T., Ghumman, W., Farrar, D., Frazier, O.: Advanced heart failure treated with continuous-flow left ventricular assist device. The New England journal of medicine **361**(23), 2241–2251 (2009)
22. Vincent, L., Soille, P.: Watersheds in digital spaces: An efficient algorithm based on immersion simulations. IEEE Transactions on Pattern Analysis and Machine Intelligence **13**, 583–598 (1991)
23. Zhang, Y., Zhan, Z., Gui, X., Sun, H., Zhang, H., Zheng, Z., Zhou, J., Zhu, X., Li, G., Hu, S., Jin, D.: Design optimization of an axial blood pump with computational fluid dynamics. ASAIO J **54**(2), 150–5 (2008)

Recent publications :

MATHEMATICS INSTITUTE OF COMPUTATIONAL SCIENCE AND ENGINEERING
Section of Mathematics
Ecole Polytechnique Fédérale
CH-1015 Lausanne

01.2012 A. ABDULLE, A. NONNENMACHER:
A posteriori error estimate in quantities of interest for the finite element heterogeneous multiscale method

02.2012 F. NOBILE, M. POZZOLI, C. VERGARA:
Time accurate partitioned algorithms for the solution of fluid-structure interaction problems in haemodynamics

03.2012 T. LASSILA, A. MANZONI, A. QUARTERONI, G. ROZZA:
Boundary control and shape optimization for the robust design of bypass anastomoses under uncertainty

04.2012 D. KRESSNER, C. TOBLER:
htucker – A Matlab toolbox for tensors in hierarchical Tucker format

05.2012 A. ABDULLE, G. VILLMART, KONSTANTINOS C. ZYGALAKIS:
Second weak order explicit stabilized methods for stiff stochastic differential equations.

06.2012 A. CABOUSSAT, S. BOYAVAL, A. MASSEREY:
Three-dimensional simulation of dam break flows.

07.2012 J BONNEMAIN, S. DEPARIS, A. QUARTERONI:
Connecting ventricular assist devices to the aorta: a numerical model.